

1 **Synthesis of 5-fluorouracil co-crystals with novel organic acids as co-formers**
2 **and its anticancer evaluation against HCT-116 colorectal cell lines**
3

4 Farhat Jubeen¹, Aisha Liaqat¹, Fiza Amjad¹, Misbah Sultan², Sania Zafar Iqbal¹, Imran Sajid³,
5 Muhammad Bilal Khan Niazi⁴, Farooq Sher^{5,*}
6

7 *1. Department of Chemistry, Government College Women University, Faisalabad 38000, Pakistan*

8 *2. Institute of Chemistry, University of the Punjab, Lahore 54590, Pakistan*

9 *3. Department of Microbiology and Molecular Genetics, University of the Punjab, Lahore 54590,*
10 *Pakistan*

11 *4. School of Chemical and Materials Engineering, National University of Sciences and*
12 *Technology, Islamabad 44000, Pakistan*

13 *5. School of Mechanical, Aerospace and Automotive Engineering, Coventry University, Coventry*
14 *CV1 5FB, UK*

15
16 *Corresponding author:

17 Email: Farooq.Sher@coventry.ac.uk; Tel: +44 (0) 24 7765 7688
18

19 **Abstract**

20 5-fluorouracil (5-FU) being a mainstream anticancer drug is under keen and detailed investigation
21 for prodrugs formulations in order to minimize the associated side effects. Co-crystallization of 5-
22 FU is an innovative technique for the synthesis of 5-FU prodrugs to improve its anticancer
23 effectiveness. The present study is based on the synthesis of 5-FU supramolecular synthons with
24 four co-formers; Succinic acid, cinnamic acid, malic acid and benzoic acid utilizing acetone as a
25 solvent. Solid state grinding followed by slow evaporation solution method was applied. Colorless
26 clear crystals were obtained in all the cases. The co-crystal formation was supported with the help
27 of FTIR and PXRD. Through FTIR, the main peaks of interest in the spectrum of 5-FU, frequency
28 (ν) of N-H (3409.02 cm^{-1}) and of carbonyl group (1647.80 cm^{-1}), were prominently shifted in all
29 the spectra of co-crystal demonstrating the replacement as well as the development of already
30 present interactions with new ones. For 5-FU-Cinnamic acid co-crystals, the anticipated peaks

31 were observed at 1673.13 cm^{-1} (-C=O) and 3566.89 cm^{-1} (N-H) manifesting significant change in
32 comparison to 5-FU. With the help of powdered XRD characterization, the representative peak of
33 5-FU was recorded at $2\theta=28.80^\circ$. The shifting of this peak and development of many new ones in
34 the spectra of co-crystals proved the development of new structural entities. Finally, the anticancer
35 activity of all the co-crystals was evaluated in comparison to that of API. All the co-crystals
36 manifest significantly greater growth inhibition potential than the main API. 5-FU-Cinnamic acid
37 (3C) was the one which proved to be the most potent anticancer agent at all the four concentrations;
38 4.82% (12 $\mu\text{g/mL}$), 34.21% (25 $\mu\text{g/mL}$), 55.08 % (50 $\mu\text{g/mL}$) and 67.29% (100 $\mu\text{g/mL}$). In short,
39 this study proved to be a true example to enhance the anticancer potential of 5-FU following fairly
40 easy fabrication requirements of co-crystallization phenomenon. After the successful synthesis of
41 these supramolecular synthons and subsequent enhancement of growth inhibition potential of 5-
42 FU, these co-crystals can further be evaluated for *in vivo* trials and membrane crossing potentials
43 in future.

44 **Keywords:** 5-fluorouracil; co-crystallization; solid state grinding method; MTT assay and
45 supramolecular interactions.

46 **1 Introduction**

47 5-FU which is simply a uracil derivative is in the exploration of many other biological activities
48 in addition to anticancer potential e.g., antimicrobial, anti-fungal, against hypertonic scars, keloids
49 and actinic keratosis etc. It is an antimetabolite of uracil obtained by the replacement of hydrogen
50 at C-5 of uracil molecule with a fluorine atom, a member of pyrimidine-based antimetabolites. 5-
51 FU is among the most common chemotherapeutic agents, introduced in 1958¹, used against a
52 variety of solid cancers by acting as thymidylate synthase inhibitor e.g., breast, colorectal, gastric,
53 head and neck cancers etc.^{2,3}. Cancer is not a single disease but a syndrome containing hundreds

54 of diseases involving rapid and uncontrolled cell growth with the potential to invade or spread to
55 the other parts of the body through the blood circulation. It is a serious public health issue around
56 the globe^{4,5}. The modern mean of cancer therapies, chemotherapy and radiation have, adversarial
57 side effects in the individuals suffering from cancer and require much dedication and work to
58 minimize the adverse outcomes⁶. The activity of 5-FU is manifested after several enzymatic
59 transformations for its binding to thymidylate synthase and its inhibition, followed by interference
60 in the synthesis of nucleic acids^{7,8}. Frequent undesirable side effects associated with 5-FU
61 chemotherapy are gastrointestinal symptoms, alopecia, cardio-toxicity and neutropenia, while
62 leuko-encephalopathy, depression, organic mental disorder⁹ have limited its clinical use; only
63 tegafur, Floxuridine, Carmofur¹⁰ are potential drugs in use.

64 Chemical modification of an active drug in order to minimize its drawbacks and to bring
65 unchanged at the targeted site is a contemporary phenomenon to obtain the desired outcomes of a
66 drug. In this regard, innumerable approaches for 5-FU structural modifications have been devised
67 and tested. 5-FU formulations in the form of nanoparticles^{11, 12, 13, 14, 15}, combination with
68 macromolecules^{4, 16}, attachment with target selective pro moieties like DNA intercalator
69 molecules^{17, 18} certainly incorporated and enhanced many vital properties of 5-FU. Following
70 these strategies; half-life of 5-FU, target selectivity and sustained blood level is enhanced.
71 However; in none of the above-mentioned approaches, synthesis methodologies are free from
72 inadequacies. There is not even a single protocol in the above-mentioned strategies which reveals
73 combined advantages of single step synthesis, easy synthesis requirements, no need for isolation
74 and purification of end products. Co-crystallization is an advanced phenomenon which combined
75 all the above-mentioned synthesis requirements in a single methodology¹⁹.

76

77 5-FU Co-crystals were successfully synthesized with some aromatic compounds; 3-
78 hydroxybenzoic acid, 4-aminobenzoic acid and cinnamic acid following grinding method. All
79 three synthesized co-crystals manifest improved membrane permeability. However, the reasons
80 behind the selection of these co-formers were not specified²⁰. Besides this, cocrystals of 5-FU are
81 also reported with heterocyclic compounds; Acridine, Phenazine and 4,4-bispyridylethene²¹ and
82 benzoic acid derivatives; 4-methylbenzoic acid and 3-aminobenzoic acid following solution
83 method. Again in none of these studies, the effectiveness of co-formers was mentioned²².
84 Although, studies are reported about the successful formation of 5-FU co-crystal with a variety of
85 co-formers with the help of their structural evidence. However, data is lacking in their biological
86 effectiveness; like, in none of these the anticancer potential of the synthesized pro moieties was
87 evaluated. In a very recent study, supramolecular synthons of 5-FU were synthesized with two
88 dihydroxybenzoic acid compounds (gentisic acid and 3,4-dihydroxybenzoic acid) and a pyridine
89 derivative (p-aminopyridine)²³. No doubt, the study was comprehensive in lieu of physical and
90 biological characterization of synthesized co-crystals. However, ethanol was used as a solvent
91 which itself is strongly capable of hydrogen bonding interactions. In a very innovative study of
92 drug plus drug co-crystals of 5-FU with 5-fluorocytocine, water was used as a solvent to develop
93 co-crystals. Water is itself capable of developing strong hydrogen bonding interactions^{24, 25}. In
94 short, some of the studies in this domain are focused only on the successful formation of co-crystals
95 without their biological evaluation. Also, in majority of the studies the reason behind the selection
96 of co-formers or the effectiveness of co-formers is not mentioned. Moreover, the solvents utilized
97 for the development of co-crystals in almost all the reported studies are capable of participating in
98 the formation of hydrogen bonding interactions.
99

100 In contrast to all reported studies; the present study aimed to utilise a solvent not having any
101 hydrogen bond donating or accepting groups. 5-FU Co-crystals are being reported with four
102 diverse co-formers; cinnamic acid (Cn), succinic acid (Sc), malic acid (MI) and benzoic acid (Bn).
103 All the co-formers were selected by keeping their individual anticancer, antioxidant and anti-
104 inflammatory properties^{26, 27, 28, 29} in consideration which could be resulted in the augmentation of
105 the overall effectiveness of 5-FU after co-crystallization. In all the reported studies in this domain,
106 methanol or water solvent was used to facilitate the development of supramolecular interactions.
107 However, in the present study, acetone, a nonpolar, aprotic solvent is used to ascertain the
108 hydrogen bonding interactions only between API and co-formers. Although acetone has partial
109 negative oxygen atom and partially positive terminal hydrogens however it does not form
110 intramolecular hydrogen bonds however intermolecular hydrogen bonding is reported but only
111 with water molecules³⁰. The co-crystal formation is analyzed with the help of FTIR and PXRD.
112 Besides this anticancer potential of all the synthesized co-crystal is evaluated with the help of MTT
113 assay. This study is a true example to further develop supramolecular interactions (non-covalent
114 interactions) of 5-FU with a variety of effective co formers and further studies can be designed
115 following the same approach utilizing a variety of suitable solvents.

116 **2 Material and methods**

117 **2.1 Materials**

118 5-FU was purchased by Sigma-Aldrich. Other chemicals in the present study were cinnamic acid
119 (VWR, 99%), succinic acid (Avandol, ultrapure), malic acid (BDH Chemicals Ltd, 99.5%),
120 benzoic acid (Duksan pure chemicals, 99.5%) and acetone (Merck KGaA, 99.5%). Co-crystals of
121 5-FU were synthesized with cinnamic acid, succinic acid, malic acid and benzoic acid following
122 solid-state grinding followed by slow evaporation solution method^{31,32, 33}.

123 **2.2 Preparation of co-crystals**

124 **2.2.1 Mechanical grinding method**

125 The equimolar quantities of API (0.572 g) and co-former (Cn, 0.162 g; Sc, 0.129 g; MI, 0.1474 g
126 and Bn, 0.1343 g), 4.4 mM, were ground strongly using motor and pestle for about 30 minutes.
127 The method employed in the study³², was followed with some modifications. The ground mass
128 was then dissolved in about 10 mL of acetone to form a solution. Afterwards, it was heated to form
129 a clear solution. Finally, the vials were cooled to room temperature and placed for a few days for
130 evaporation to observe crystal formation. In all cases, Colourless crystals were obtained.

131 **2.3 Characterization**

132 **2.3.1 FTIR and PXRD**

133 The development of supramolecular interactions as a consequence of practical changes in
134 vibrational modes of anticipated functional groups were evaluated with the help of FTIR analysis.
135 This characterization was done at ATR-FTIR spectrophotometer (Shimadzu IR prestige-21, USA).
136 Transmission mode in the range of 400 cm⁻¹ to 4000 cm⁻¹ was applied to record the spectra. The
137 study of all the Spectra was done in comparison to the API spectrum alone and the difference
138 absorption frequencies of -N-H and -C=O groups from the observed place and shape (position at
139 which the peak was observed in the spectrum of API alone) were evaluated in order to study the
140 formation of non-covalent interactions for the synthesis of co-crystals³⁴. For further confirmation
141 of new hydrogen bonding interactions, co-crystals were analysed through PXRD^{20, 34, 35}. PXRD
142 analysis is based on constructive interference between homochromatic X-rays and crystalline
143 samples. During this procedure, X-rays were formed by cathode ray tube. These rays were then

144 filtered to get homochromous rays, accumulated and then focused towards the sample. Finally, the
145 bio-evaluation of the as prepared co-crystals was done through MTT assay ^{36,37}.

146 **2.3.2 MTT assay *In vitro***

147 For the evaluation of antitumor potential of synthesized co-crystals, Human colorectal cancer cell
148 lines (HCT 116) ATCC®CCL-247™ [(catalogue no: 91091005-1VL) Sigma Aldrich] were utilized.
149 Cultivation of cells in the form of a monolayer was performed in T-75 flasks Costar and the
150 subculturing was done two times a week. The conditions were; 37 °C in CO₂ (5%) and 100%
151 relative humidity provided incubator. The passage number was kept low, from 5 to 20, for the
152 accomplishment of this process. The medium applied for the cultivation of HCT 116 was McCoy's
153 5A Gibco Glasgow, complemented with fetal bovine serum (FBS) (10%), Gibco, Glasgow, UK
154 and antibiotics (1%) (streptomycin, penicillin)³⁸.

155
156 Washing of the anchorage-dependent cells at an exponential growth phase was performed with
157 PBS (phosphate buffered saline) about 2 mL. Subsequently, the separation was done with the help
158 of 0.5 mL of 1X trypsin and reared for 2–5 minutes at 37 °C in the incubator. About 100 µL of
159 complete growth media was poured into 96-well flat-bottom microplates per well. Afterwards, the
160 calculation of cells was performed for anticipated densities with the help of staining using trypan
161 blue and tallied with a hemacytometer. Densities of 1,000–100,000 cells per well were injected³⁷.
162 Subsequently, cells were treated with a range of concentrations of synthesized co-crystals; 12, 25,
163 50 and 100 mg/mL. The experiments were performed in triplicates to avoid errors.

164
165 Further in each experiment Background control wells having the same volume of complete culture
166 medium were involved accompanied by a positive control comprising Triton X-100 and negative

167 controls as well. Then the plate was cultivated at 37 °C for 24 hours in CO₂ supplied moistened
168 incubator³⁹. 3-(4, 5-dimethyl thiazol-2-yl)-2, 5-diphenyl tetrazolium bromide (MTT) (10 µL) was
169 directly supplemented in the culture media of each well after 24 hours. Then incubation of the
170 plate was performed for about 4 hours at 37 °C in 5% CO₂ incubator. After incubation, the
171 separation of culture media was done softly so that the cell's monolayer remains intact.
172 Afterwards, each well was) supplemented with 100 µL volume of dimethyl sulfoxide (DMSO) in
173 each well and plate was shaken to homogenize formazan⁴⁰. Absorbance was evaluated with the
174 help of spectrophotometer at 570 nm wavelength. The anticancer potential was found out by the
175 calculation of inhibition rate and graphs were plotted against all concentrations. Finally, for each
176 extract. IC₅₀ values were calculated. The growth inhibition rate was calculated using Eq. (1) ⁴¹:

177

$$178 \quad \text{Percentage Mortality (\%)} = \frac{\text{O.D (Control well)} - \text{O.D (Treated well)}}{\text{O.D (Control well)}} \times 100 \quad (1)$$

179

180 where O.D is optical density.

181 **3 Results and discussion**

182 **3.1 Verification of supramolecular interactions**

183 This phenomenon is based on the fact, that different chemical bonds and functional groups having
184 several vibrational modes absorb in the infrared region and have characteristic absorption peaks.
185 FTIR analysis was done to observe the variations in the vibrational modes of functional groups as
186 a consequence of new supramolecular interactions. Spectra of co-crystals of API and co- former
187 were studied comparatively to the spectrum of API alone and shifting of different peaks such as
188 N-H and C=O, from peaks of API spectrum were due to involvement of these groups in hydrogen
189 bonding between them. Absorption frequencies of 5-FU, all the co formers and co-crystals are

190 represented in Table 1. In the IR spectrum of unsubstituted or non-derivatized 5-FU, a rounded
191 peak at 3409.02 cm^{-1} can be accredited to the absorption frequency of (N-H) group (stretching)
192 and a wide sharp band of high intensity at wavenumber, 1647.77 cm^{-1} can be assigned to $\nu(\text{C}=\text{O})$
193 groups (stretching)^{42, 43}.

194 3.1.1 5-FU-Cinnamic acid (5-FU-Cn)

195 For the development of 5-FU supramolecular synthones with Cinnamic acid; the already present
196 $-\text{N}-\text{H}\dots\text{N}-\text{H}$ interactions were supposed to be replaced by $-\text{N}-\text{H}\dots\text{O}-\text{H}$ or $-\text{N}-\text{H}\dots\text{O}=\text{C}$ as shown
197 in Figure 2. The larger molecule of cinnamic acid is associated with enhanced steric hindrance.
198 This leads to weaker supramolecular interactions. These weak intermolecular interactions result in
199 strong intramolecular interactions, therefore; it was expected that $-\text{N}-\text{H}$ groups will absorb at an
200 increased stretching frequency. Noninvolvement of molecules in the supramolecular interactions
201 are reduced stretching of intramolecular bonds and in turn increase strength. The observation of
202 $3432.03, 3566.89\text{ cm}^{-1}$ peaks in the spectrum of co-crystal with a significant blue shift, as clear
203 from Figure 1, is supporting the successful synthesis of co-crystals and in an agreement with the
204 results of Nadzri *et al.*,³³. This observation is further supported by the shift of $-\text{C}-\text{N}$ absorption
205 frequency towards shorter wavelength (blue shift). In the spectrum of 5-FU, the $\nu(-\text{C}-\text{N})$ was
206 observed at 1242.00 cm^{-1} which shifted hypochromially at 1252.47 in the spectrum of 5-FU-Cn
207 supramolecular synthons³⁸. On the other hand, the trend of absorption frequency of $-\text{C}=\text{O}$ groups
208 at 1673.13 cm^{-1} is according to the trend reported in the literature³³ following hypochromic shift.
209 Again, the increased strengthening of $-\text{C}=\text{O}$ bond may be the consequence of increased steric
210 hindrance and bigger molecular size of co-former also proposed in Figure 2. This is also proved
211 true after the peak at 1179.10 cm^{-1} ($-\text{C}-\text{O}$)⁴² in the 5-FU spectrum diminished in the co-crystal

212 spectrum due to the vanished single bond properties of carbonyl groups in the course of co-crystal
213 formation.

214 **3.1.2 5-FU-Succinic acid (5-FU-Sc)**

215 The –N-H absorption frequency for 5-FU-Sc co-crystals was observed at 3543.53 cm^{-1} clear from
216 Figure 4 that manifesting the same blue shift as discussed for the above case exactly in accordance
217 with Nadzri *et al.*,³³. Moreover, this observation can also be justified by the same trend of a blue
218 shift in the absorption frequencies of -C-N groups; 1346.62 cm^{-1} (5-FU) and 1437.33 cm^{-1} (5-FU-
219 Sc)³⁸.

220 The absorption frequency of carbonyl groups was observed at 1644.51 cm^{-1} . This frequency seems
221 to be almost at the same frequency in comparison to that of un-substituted API and
222 bathochromially shifted as compared to the co-former²³ as shown in Figure 3. Moreover, the
223 absorption frequencies of -C-O were also observed at almost same positions; 1179.10 cm^{-1} (5-FU)
224 and 1174.75 cm^{-1} (5-FU-Sc)⁴². This suggests the efficient involvement of carbonyl groups of co-
225 former in the development of hydrogen bonding interaction as compared to 5-FU. This may be the
226 result of more steric hindrance of the cyclic structure of 5-FU than the aliphatic structure of
227 succinic acid as depicted in Figure 4.

228 **3.1.3 5-FU-Maleic acid (5-FU-MI)**

229 Following the usual hypochromic shift^{20, 34}, the –N-H absorption frequency of 5-FU-MI co-
230 crystals was detected at 3492.20 cm^{-1} , observed from the spectra Figure 5, clearly demonstrating
231 the development of new supramolecular interactions as anticipated in Figure 6. As the maleic acid
232 has almost the same structure as succinic acid, therefore, a same trend of absorption of carbonyl
233 was observed. This frequency of carbonyl groups was recorded at 1669.96 cm^{-1} (Figure 5); strongly

234 red shifted as compared to co-former and reverse is true in comparison to API. This observed trend
235 is also affirmed by the observation of -C-O absorption frequencies of API and co-crystals at the
236 shift of less than 10 cm^{-1} (non-significant); 1179.10 cm^{-1} (5-FU) and 1080.89 cm^{-1} (5-FU-MI) ⁴².
237 This suggests the strong disturbance and involvement of carbonyl groups of co-former molecules
238 while the very less involvement of carbonyl groups of API in the formation of non-covalent
239 interactions between API and Co-former for the development of co-crystals. This could be
240 explained by the bigger molecular size of malic acid that generates high steric hindrance while
241 forming hydrogen bonds with the consecutive NH-CO-NH groups of 5-FU as manifested in Figure
242 6.

243 **3.1.4 5-FU-Benzoic acid (5-FU-Bn)**

244 The absorption frequency of -N-H group was observed at 3431.72 cm^{-1} with regular hypochromic
245 shift and the frequency of -C=O was found at 1672.37 cm^{-1} (Figure 7). The hypochromic shift of
246 -N-H group was further tallied with the same shift of -C-N group frequency. Absorption frequency
247 of -C-N in the 5-FU spectrum was observed at 1242.00 cm^{-1} while this group in the co-crystal
248 spectrum shown their IR absorption at 1284.12 cm^{-1} ³⁸. On the other hand, the carbonyl group
249 frequency of 5-FU at 1647.77 cm^{-1} is missing in the co-crystal spectrum. As the 1672.37 cm^{-1} is
250 matching with $\nu(\text{C}=\text{O})$ of co-former (1674.98 cm^{-1}), therefore; it could be proposed that the double
251 bond character of the carbonyl group of 5-FU was diminished as a result of strong involvement of
252 this group for the development of supramolecular interactions. Both these frequencies followed
253 the same trend as discussed above for all the other co-crystal forms. The proposed hydrogen
254 bonding interactions which could be developed are represented in Figure 8. In short, in all the co-
255 crystal forms, significant shifts in absorption frequencies of anticipated peaks with almost the same

256 trends were observed. The observed trends in all the cases are in the favour of an effective
257 formation of new non-covalent interactions.

258 **3.2 Distinction of API and co-crystals` structure by PXRD**

259 Once the development of supramolecular interactions was clearly recognized through FTIR
260 analysis, the formation of co-crystals was supplementarily indorsed with the help of PXRD. The
261 intensity, 2θ values, FWHM (full width at half maximum) values of most protruding peaks and
262 crystal size of API and all the co-crystals are arranged in Table 2. The values of intensity are
263 representative of preferred orientation as well as crystallinity of molecules. FWHM not only
264 provides the comparison of data distribution under the curve of most prominent peaks but is also
265 important to find out the crystal size. The characteristic peaks in the spectrum of 5-FU are clearly
266 different from the respective peaks in the co-crystal spectra in all the above-mentioned aspects as
267 well as crystal size. These differences are observable with respect to both the shapes and the
268 intensity of the peaks as manifested in Figure 9. These differences are obviously suggestive of the
269 changes in the structural properties of API as a consequence of the changes in supramolecular
270 interactions with different co-formers ^{34, 44}.

271
272 It is observable from the API and co-crystals` stacked graph in Figure 9, the peak observed at 2θ
273 $=28.80^\circ$, precisely the same as stated in ³⁴, is the most strong representative peak of 5-FU. This
274 illustrative value of 5-FU appeared to be prominently different from the values observed in all the
275 graphs of co-crystals ²³. For 5-FU-Cn co-crystals the most prominent, intense peak appeared at
276 27.78° . The intensity of this peak is lesser than the most prominent peak of API manifesting
277 decreased preferred orientation and in turn, reduced crystallinity. Similarly, in the case of 5-FU-
278 Sc co-crystals the intensity of most prominent peak is very low in comparison to that of API

279 demonstrating the very small preferred orientation and lessened crystallinity. This finding is also
280 supported by the strongest (-N-H) stretching frequencies of 5-FU-Cn and 5-FU-Sc co-crystals with
281 the help of FTIR analysis that manifests the strengthening of intramolecular interactions as a
282 consequence of weakening of intermolecular interactions as a result of the intervention of co-
283 former molecules. This resulted in the disturbance of already present supramolecular interactions
284 in 5-FU crystal structure due to the development of interactions between 5-FU and co-former
285 molecules. Moreover, the crystal size of 5-FU-Sc and 5-FU-Cn co-crystals is smaller than the size
286 of API manifesting the formation of co-crystals in the amorphous form ⁴⁵.

287
288 While if we Consider 5-FU-MI and 5-FU-Bn co-crystals, both have their most prominent peaks at
289 28.72 ° and almost matching and very high intensities. This observation is revealing much
290 enhanced crystallinity as a result of very high preferred orientation. The crystal size of both of
291 these co-crystals is much bigger than the 5-FU crystal size. The observation of almost similar peaks
292 in 5-FU-MI and 5-FU-Bn co-crystals may be as a consequence of the same type of groups
293 responsible for hydrogen bonding interactions in the same directions. Moreover; the crystal size
294 of both the co- formers are almost the same. Besides these facts, there are many other peaks in the
295 spectrum of 5-FU which are missing in all the spectra of co-crystals also clear from Figure 9.
296 Furthermore, in all the four spectra of co-crystals, many new peaks are found which are indicative
297 of the formation of entirely new and different structural entities than 5-FU ³⁴. From all the four co-
298 crystal forms; 5-FU-MI and 5-FU-Bn proved to be the entities with the highest crystallinity, having
299 bigger crystallite size than the other two co-crystals.

300 **3.3 Assessment of Anticancer potential of co-crystals through MTT assay**

301 Table 3 incorporates the values of percent growth inhibition of actinomycetes *in vitro* at four
302 different concentrations in HCT-116 colorectal cell lines, after application of 5-FU alone and all
303 the four co-crystals of 5-FU³⁷. For the evaluation of the most effective growth inhibiting agent,
304 values are represented comparatively in Figure 10 to Figure 13. It is clear from the observed values
305 that as the concentration of actinomycetes is increased, the value of percent growth inhibition is
306 also increased and maximum growth inhibition is observed at 100 ug/mL for API and all the co-
307 crystals. This trend is quite rational as the increased concentration of actinomycetes provides
308 increased substrate sites for the applied agents to execute and subsequently the numerical value of
309 growth inhibition is also increased.

310
311 After a comparison of all the co-crystals, it is clear that 5-FU-Cn co-crystals proved to be the
312 highest growth inhibiting agents at all the four concentrations. At 100 µg/mL concentration, the
313 growth inhibiting potential of 5-FU-Cn co-crystals is 67.30%, highest among all the synthesised
314 supramolecular synthons. The reason behind this observation may be the anticancer potential of
315 cinnamic acid itself. Cinnamic acid derivatives were widely studied and employed as potent
316 antitumor agents. The α,β -unsaturated carbonyl moiety in cinnamic acid is considered as an active
317 site utilized for the design of anticancer drugs⁴⁶. The other most important reason also evident
318 from the FTIR and PXRD analysis is the loose bonding (FTIR) and less crystallinity (PXRD) of
319 5-FU-Cn co-crystals, resulted in easy release of API and co-former molecules and their prompt
320 action. The second most potent anticancer agent as clear from the values of Table 3 are 5-FU-Bn
321 co-crystals at all the four concentrations; 66.92% growth inhibition at 100 µg/mL. While the 5-
322 FU-Ml and 5-FU-Sc cocrystals have mixed trend. However, at 100 µg/mL, 5-FU-Ml acid has

323 greater growth inhibition, 44.55% than 5-FU-Sc (38.91%). The reason behind this variable end
324 observed for 5-FU-Sc and 5-FU-MI co-crystals is not clear. Dissimilar growth inhibiting strengths
325 of API and all the co-crystals may be attributed to a different structural characteristic of co-formers
326 and diverse interactions between API and co-formers.

327 **4 Conclusion**

328 Four different co-crystals were synthesized following the solid state grinding followed by normal
329 slow evaporation solvent method. The solvent used in this study to facilitate supramolecular
330 interactions was acetone; not used before in any study on a similar concept. Co-crystals were
331 successfully formed in all four cases at room temperature. FTIR and PXRD analysis of API and
332 cocrystals clearly indicated the development of hydrogen bonding interactions between API and
333 all the co-formers. In the FTIR spectrum of 5-FU, the absorption frequencies of main anticipated
334 peaks that is N-H and -C=O were found at 3409.02 cm^{-1} and 1647.77 cm^{-1} respectively. Both of
335 these peaks were clearly shifted in all the spectra of co-crystals exactly according to the trends
336 reported in the literature. These shifts were clearly indicative of alterations in the intermolecular
337 interactions of 5-FU molecules as a consequence of intervention of co-former molecules.
338 Moreover, in the PXRD spectrum, the most prominent peak of 5-FU was recorded at $2\theta = 28.80$.
339 This peak was not detected in any spectrum of co-crystals; further, in all the spectra of co-crystals
340 many new peaks were recorded manifesting the development of entirely different moieties after
341 co-crystallization. After the successful formation of co-crystals in all the four cases, their
342 anticancer effectiveness was evaluated utilizing HCT-116 colorectal cell lines at four different
343 concentrations of synthesized co-crystals. All the four co-crystals proved to be more effective than
344 API alone at all the four concentrations. Moreover, 5-FU-Cn (3C) co-crystals at 100 ug/mL proved
345 to be the most potent anticancer agent in this study. In short, this study proved the formation of

346 compelling prodrugs of 5-FU following very easy synthesis procedure and conditions. As this
347 method is quite captivating from the point of view of its tireless synthesis requirements and diligent
348 outcomes; these co-crystals can be further optimized for their *in vivo* safety. Moreover; many other
349 potentially effective co-formers could also be studied in future.

350

- 352 (1) Longley, D. B.; Harkin, D. P.; Johnston, P. G., 5-fluorouracil: mechanisms of action and
353 clinical strategies. *Nat. Rev. Cancer* **2003**, 3, 330-8.
- 354 (2) Chandran, S. P.; Natarajan, S. B.; Chandraseharan, S.; Mohd Shahimi, M. S. B., Nano drug
355 delivery strategy of 5-fluorouracil for the treatment of colorectal cancer. *J. Cancer Res. Pract.*
356 **2017**, 4, 45-48.
- 357 (3) da Silva, C. C. P.; de Oliveira, R.; Tenorio, J. C.; Honorato, S. B.; Ayala, A. P.; Ellena, J.,
358 The Continuum in 5-Fluorocytosine. Toward Salt Formation. *Cryst. Growth Des.* **2013**, 13, 4315-
359 4322.
- 360 (4) Zhang, Z.; Zhang, Q.; Wang, J.; Shi, X.; Zhang, J.; Song, H., Synthesis and drug release in
361 vitro of porphyrin carrying 5-Fluorouracil. *Carbohydr.* **2010**, 79, 628-632.
- 362 (5) Nisa, Z. U.; Zafar, A.; Sher, F., Assessment of knowledge, attitude and practice of adverse
363 drug reaction reporting among healthcare professionals in secondary and tertiary hospitals in the
364 capital of Pakistan. *Saudi. Pharm. J.* **2018**, 26, 453-461.
- 365 (6) Jubeen, F.; Liaqat, A.; Sultan, M.; Iqbal, S. Z.; Sajid, I.; Sher, F., Green synthesis and
366 biological evaluation of novel 5-fluorouracil derivatives as potent anticancer agents. *Saudi Pharm.*
367 *J.* **2019**, 27, 1164-1173.
- 368 (7) Fernandes, E.; Ferreira, D.; Peixoto, A.; Freitas, R.; Relvas-Santos, M.; Palmeira, C.;
369 Martins, G.; Barros, A.; Santos, L. L.; Sarmiento, B.; Ferreira, J. A., Glycoengineered nanoparticles
370 enhance the delivery of 5-fluorouracil and paclitaxel to gastric cancer cells of high metastatic
371 potential. *Int. J. Pharm.* **2019**, 570, 118646.
- 372 (8) Chakraborty, P.; Dastidar, P., An easy access to topical gels of an anti-cancer prodrug (5-
373 fluorouracil acetic acid) for self-drug-delivery applications. *Chem. Commun.* **2019**, 55, 7683-7686.
- 374 (9) Radwan, A.; Alanazi, F., Design and synthesis of new cholesterol-conjugated 5-
375 fluorouracil: a novel potential delivery system for cancer treatment. *Molecules.* **2014**, 19, 13177-
376 13187.
- 377 (10) Ulaiwy, M. A. A.; Hadi, M. K.; Farhan, M. S.; Khudhair, A. R., Synthesis and Antitumor
378 Evaluation of Some 5-fluorouracil Derivatives. *Der. Pharm. Chemica.* **2017**, 9, 101-106.
- 379 (11) Tummala, S.; Satish Kumar, M. N.; Prakash, A., Formulation and characterization of 5-
380 Fluorouracil enteric coated nanoparticles for sustained and localized release in treating colorectal
381 cancer. *Saudi. Pharm. J.* **2015**, 23, 308-14.
- 382 (12) Subudhi, M. B.; Jain, A.; Jain, A.; Hurkat, P.; Shilpi, S.; Gulbake, A.; Jain, S. K., Eudragit
383 S100 Coated Citrus Pectin Nanoparticles for Colon Targeting of 5-Fluorouracil. *Materials.* **2015**,
384 8, 832-849.
- 385 (13) Abd-Rabou, A. A.; Bharali, D. J.; Mousa, S. A., Taribavirin and 5-Fluorouracil-Loaded
386 Pegylated-Lipid Nanoparticle Synthesis, p38 Docking, and Antiproliferative Effects on MCF-7
387 Breast Cancer. *Pharm. Res.* **2018**, 35, 76.
- 388 (14) Rizvi, S. A. A.; Saleh, A. M., Applications of nanoparticle systems in drug delivery
389 technology. *Saudi Pharm. J.* **2018**, 26, 64-70.
- 390 (15) Lollo, G.; Matha, K.; Bocchiardo, M.; Bejoud, J.; Marigo, I.; Virgone-Carlotta, A.;
391 Dehoux, T.; Rivière, C.; Rieu, J.-P.; Briançon, S., Drug delivery to tumours using a novel 5-FU
392 derivative encapsulated into lipid nanocapsules. *J. Drug Target.* **2019**, 27, 634-645.
- 393 (16) Alomrani, A.; Badran, M.; Harisa, G. I.; Alshehry, M.; Alhariri, M.; Alshamsan, A.;
394 Alkholief, M., The use of chitosan-coated flexible liposomes as a remarkable carrier to enhance

395 the antitumor efficacy of 5-fluorouracil against colorectal cancer. *Saudi. Pharm. J.* **2019**, 27, 603-
396 611.

397 (17) Silva, V. R.; Corrêa, R. S.; Santos, L. d. S.; Soares, M. B. P.; Batista, A. A.; Bezerra, D.
398 P., A ruthenium-based 5-fluorouracil complex with enhanced cytotoxicity and apoptosis induction
399 action in HCT116 cells. *Sci. Rep.* **2018**, 8, 288.

400 (18) Karayildirim, Ç. K.; Kotmakçı, M.; Halay, E.; Ay, K.; Başpınar, Y., Formulation,
401 characterization, cytotoxicity and Salmonella/microsome mutagenicity (Ames) studies of a novel
402 5-fluorouracil derivative. *Saudi Pharm. J.* **2018**, 26, 369-374.

403 (19) Stoler, E.; Warner, J. C., Non-covalent derivatives: cocrystals and eutectics. *Molecules.*
404 **2015**, 20, 14833-14848.

405 (20) Dai, X.-L.; Li, S.; Chen, J.-M.; Lu, T.-B., Improving the Membrane Permeability of 5-
406 Fluorouracil via Cocrystallization. *Cryst. Growth Des.* **2016**, 16, 4430-4438.

407 (21) Delori, A.; Eddleston, M. D.; Jones, W., Cocrystals of 5-fluorouracil. *Cryst. Eng. Comm.*
408 **2013**, 15, 73-77.

409 (22) Mohana, M.; Muthiah, P. T.; McMillen, C. D., Supramolecular hydrogen-bonding patterns
410 in 1: 1 cocrystals of 5-fluorouracil with 4-methylbenzoic acid and 3-nitrobenzoic acid. *Acta Cryst.*
411 *Sect. C: Struct. Chem.* **2017**, 73, 259-263.

412 (23) Gautam, M. K.; Besan, M.; Pandit, D.; Mandal, S.; Chadha, R., Cocrystal of 5-Fluorouracil:
413 Characterization and Evaluation of Biopharmaceutical Parameters. *AAPS PharmSciTech.* **2019**,
414 20, 149.

415 (24) Da Silva, C. C. P.; de Melo, C. C.; Souza, M. S.; Diniz, L. F.; Carneiro, R. L.; Ellena, J.,
416 5-Fluorocytosine/5-Fluorouracil Drug-Drug Cocrystal: a New Development Route Based on
417 Mechanochemical Synthesis. *J. Pharm. Sci.* **2018**, 14, 50-56.

418 (25) Du, Y.; Cai, Q.; Xue, J.; Zhang, Q.; Qin, D., Structural investigation of the cocrystal formed
419 between 5-fluorocytosine and fumaric acid based on vibrational spectroscopic technique.
420 *Spectrochim. Acta A. Mol. Biomol. Spectrosc.* **2017**, 178, 251-257.

421 (26) Nakamura, N.; Hirakawa, A.; Gao, J. J.; Kakuda, H.; Shiro, M.; Komatsu, Y.; Sheu, C. C.;
422 Hattori, M., Five new maleic and succinic acid derivatives from the mycelium of *Antrodia*
423 *camphorata* and their cytotoxic effects on LLC tumor cell line. *J. Nat. Prod.* **2004**, 67, 46-8.

424 (27) Subramanian, R.; Neethirajan, K.; Ramaraj, J., Profile of bioactive compounds in
425 *Syzygium cumini* – a review. *J. Pharm. Res.* **2013**, 20125, 4548-4553.

426 (28) Evans, W. C., Oxidation of phenol and benzoic acid by some soil bacteria. *Biochem. J.*
427 **1947**, 41, 373-382.

428 (29) Sharma, P., Cinnamic acid derivatives: A new chapter of various pharmacological
429 activities *J. Chem. Pharm.* **2011**, 3, 403-423.

430 (30) Fonseca, T. L.; Coutinho, K.; Canuto, S., Hydrogen bond interactions between acetone and
431 supercritical water. *Phys. Chem. Chem. Phys.* **2010**, 12, 6660-6665.

432 (31) da Silva, C. C. P.; Pepino, R. d. O.; de Melo, C. C.; Tenorio, J. C.; Ellena, J., Controlled
433 Synthesis of New 5-Fluorocytosine Cocrystals Based on the pKa Rule. *Cryst. Growth Des.* **2014**,
434 14, 4383-4393.

435 (32) Sonawane, R. P., Green synthesis of pyrimidine derivative. *Int. Lett. Chem., Phy. Astron.*
436 **2014**, 2, 64-68.

437 (33) Nadzri, N. I.; Sabri, N. H.; Lee, V. S.; Halim, S. N. A., 5-fluorouracil co-crystals and their
438 potential anti-cancer activities calculated by molecular docking studies. *J. Chem. Crystallogr.*
439 **2016**, 46, 144-154.

- 440 (34) Moisescu-Goia, C.; Muresan-Pop, M.; Simon, V., New solid state forms of antineoplastic
441 5-fluorouracil with anthelmintic piperazine. *J. Mol. Stru.* **2017**, 1150, 37-43.
- 442 (35) Li, S.; Chen, J.-M.; Lu, T.-B., Synthon polymorphs of 1: 1 co-crystal of 5-fluorouracil and
443 4-hydroxybenzoic acid: their relative stability and solvent polarity dependence of grinding
444 outcomes. *Cryst. Eng. Comm.* **2014**, 16, 6450-6458.
- 445 (36) Petaccia, M.; Condello, M.; Giansanti, L.; La Bella, A.; Leonelli, F.; Meschini, S.; Villalva,
446 D. G.; Pellegrini, E.; Ceccacci, F.; Galantini, L., Correction: Inclusion of new 5-fluorouracil
447 amphiphilic derivatives in liposome formulation for cancer treatment. *Med. Chem. Comm.* **2016**,
448 7, 378-378.
- 449 (37) Fang, F.-Q.; Guo, H.-S.; Zhang, J.; Ban, L.-Y.; Liu, J.-W.; Yu, P.-Y., Anti-cancer effects
450 of 2-oxoquinoline derivatives on the HCT116 and LoVo human colon cancer cell lines. *Mol. Med.*
451 *Rep.* **2015**, 12, 8062-8070.
- 452 (38) Dhanavel, S.; Revathy, T.; Sivaranjani, T.; Sivakumar, K.; Palani, P.; Narayanan, V.;
453 Stephen, A., 5-Fluorouracil and curcumin co-encapsulated chitosan/reduced graphene oxide
454 nanocomposites against human colon cancer cell lines. *Polym. Bull.* **2020**, 77, 213-233.
- 455 (39) Vichai, V.; Kirtikara, K., Sulforhodamine B colorimetric assay for cytotoxicity screening.
456 *Nat. Protoc.* **2006**, 1, 1112.
- 457 (40) Sanjay, P.; Nirav, G.; Ashok, S.; Anand, S., In-Vitro cytotoxicity activity of Solanum
458 Nigrum Extract against Hela cell line and Vero cell line. *Int. J. Pharm. Pharm. Sci.* **2009**, 1, 38-
459 46.
- 460 (41) Shahneh, F. Z.; Valiyari, S.; Azadmehr, A.; Hajiaghaee, R.; Yaripour, S.; Bandehagh, A.;
461 Baradaran, B., Inhibition of Growth and Induction of Apoptosis in Fibrosarcoma Cell Lines by
462 Echinophora platyloba DC: In Vitro Analysis. *Adv. Pharmacol. Sci.* **2013**, 2013, 7.
- 463 (42) Chen, P.-C.; Yii, D.; Tsai, H.-C.; Parasuraman, V. R.; Prasannan, A.; Kao, C.-Y.; Lai, J.-
464 Y., Fabrication of branched polyethylenimin/alginate/poly(cyclohexane-1,4-diyl acetone
465 dimethylene ketal as a nano size carrier for controlled release of 5-fluorouracil. *React. Funct.*
466 *Polym.* **2019**, 145, 104238.
- 467 (43) Abdelghani, E.; Said, S. A.; Assy, M.; Hamid, A. M. A., Synthesis and antimicrobial
468 evaluation of some new pyrimidines and condensed pyrimidines. *Arab. J. Chem.* **2017**, 10, S2926-
469 S2933.
- 470 (44) Sugiyama, H.; Johmoto, K.; Sekine, A.; Uekusa, H., Reversible on/off switching of
471 photochromic properties in N-salicylideneaniline co-crystals by heating and humidification. *Cryst.*
472 *Eng. Comm.* **2019**, 21, 3170-3175.
- 473 (45) Roy, D.; James, S. L.; Crawford, D. E., Solvent-free sonochemistry as a route to
474 pharmaceutical co-crystals. *Chem. Commun.* **2019**, 55, 5463-5466.
- 475 (46) P., D.; Baltas, M.; Belval, F. B., Cinnamic Acid Derivatives as Anticancer Agents-A
476 Review *Curr. Med. Chem.* **2011**, 18, 1672-1703
477

478

List of Tables

479

Table 1. FTIR absorption frequencies of the main peaks of interest.

Sample ID	ν (C=O) cm^{-1}	ν (N-H) str cm^{-1}
5-FU	1647.77	3409.02
5-FU-Cn (3C)	1673.13	3432.03, 3566.89
Cn (3)	1668.29	-
5-FU-Sc (4C)	1644.51	3543.53
Sc (4)	1676.04	-
5-FU-MI (5C)	1669.96	3492.20
MI (5)	1688.89	-
5-FU-Bn (6C)	1672.37	3431.72
Bn (6)	1674.98	-

480

481

482

483 **Table 2.** 2θ , FWHM and crystallite size of 5-FU and co-crystals using Scherrer equation.

Sample ID	Intensity	2θ in Θ	θ in Θ	Cos θ	FWHM	Crystallite	
	In counts	Degrees	Radians			Size (\AA°)	
5-FU	1156	28.80°	14.40	0.25	0.969	0.24	5.96
5-FU-Ch (3C)	1086.54	27.78°	13.89	0.24	0.971	0.32	4.41
5-FU-Sc (4C)	787.92	28.78°	14.39	0.25	0.969	0.25	5.79
5-FU-MI (5C)	4544.86	28.72°	14.36	0.25	0.969	0.16	8.74
5-FU-Bn (6C)	4529.28	28.72°	14.36	0.25	0.969	0.17	8.74

484

485

486 **Table 3.** Percentage growth inhibition in HCT-116 cell lines using different concentrations of API
487 and Synthesized co-crystals.

Sample ID	Concentrations of actinomycetes			
	12 µg/mL	25 µg/mL	50 µg/mL	100 µg/mL
5FU	7.89±0.64	16.21±0.20	39.53±0.56	54.28±0.56
3C	24.81±0.42	34.21±0.41	55.08±0.53	67.29±1.73
4C	14.85±0.57	18.42±0.42	32.89±0.50	38.91±0.51
5C	9.97±0.90	26.13±0.53	31.02±0.58	44.55±0.57
6C	23.31±0.58	29.89±0.65	53.57±0.33	66.92±0.63

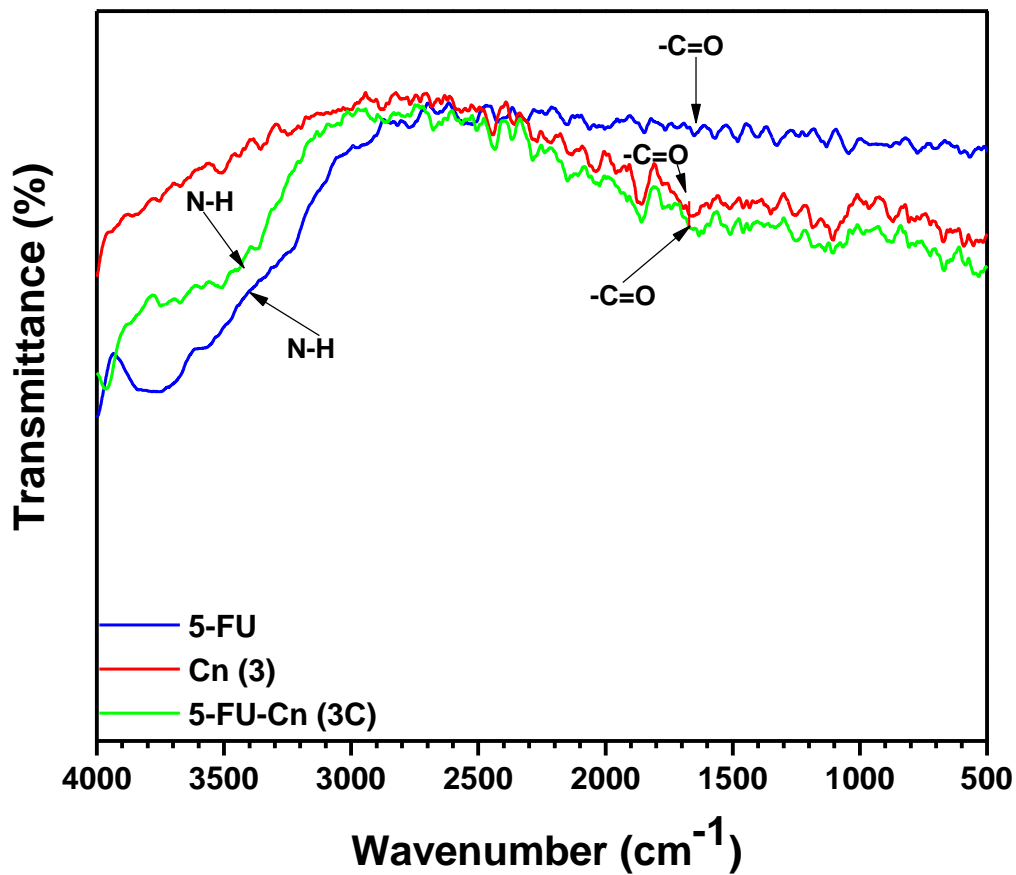
488

489

List of Figures

490

491



492

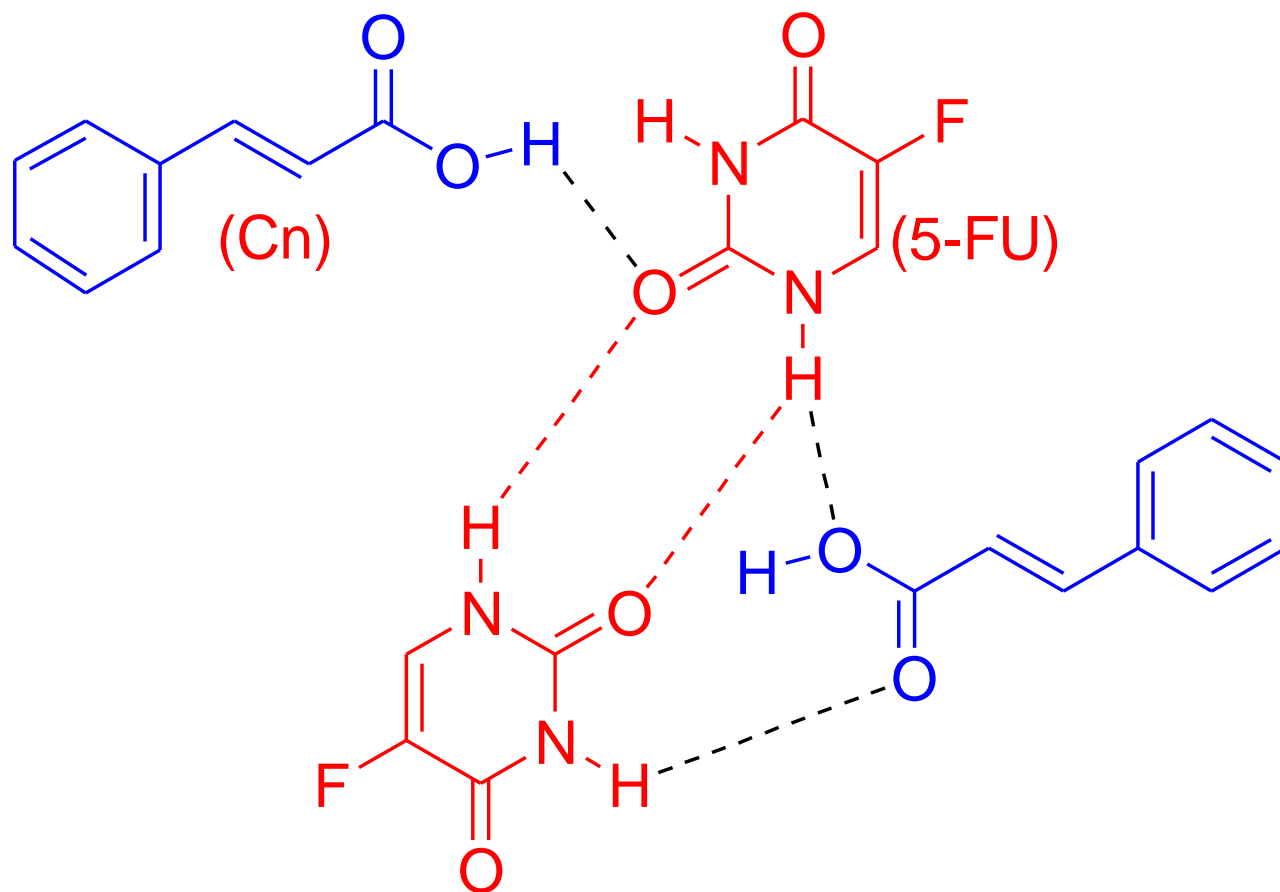
493 **Figure 1.** IR spectra of 5-FU, Cn (Cinnamic acid) co-former and 5-FU-Cn co-crystals.

494

495

496

497



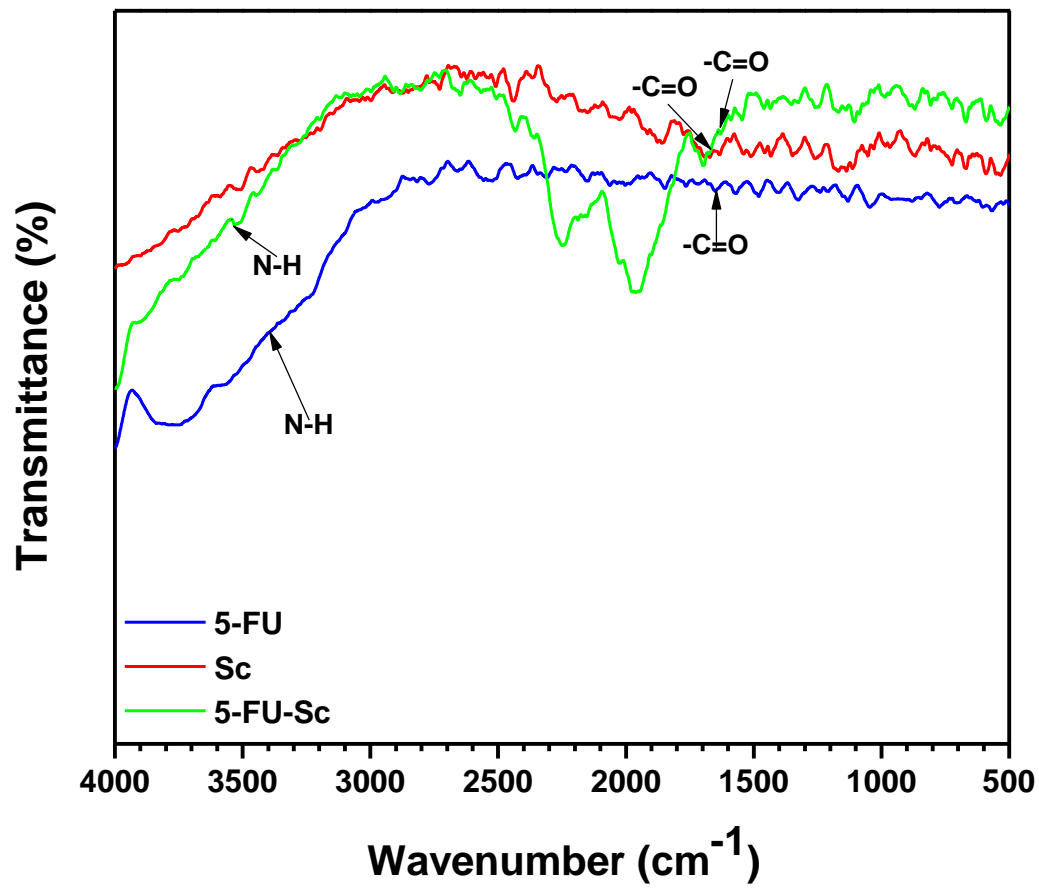
498

499

500

Figure 2. Proposed supramolecular interactions in 5-FU-Cn co-crystals.

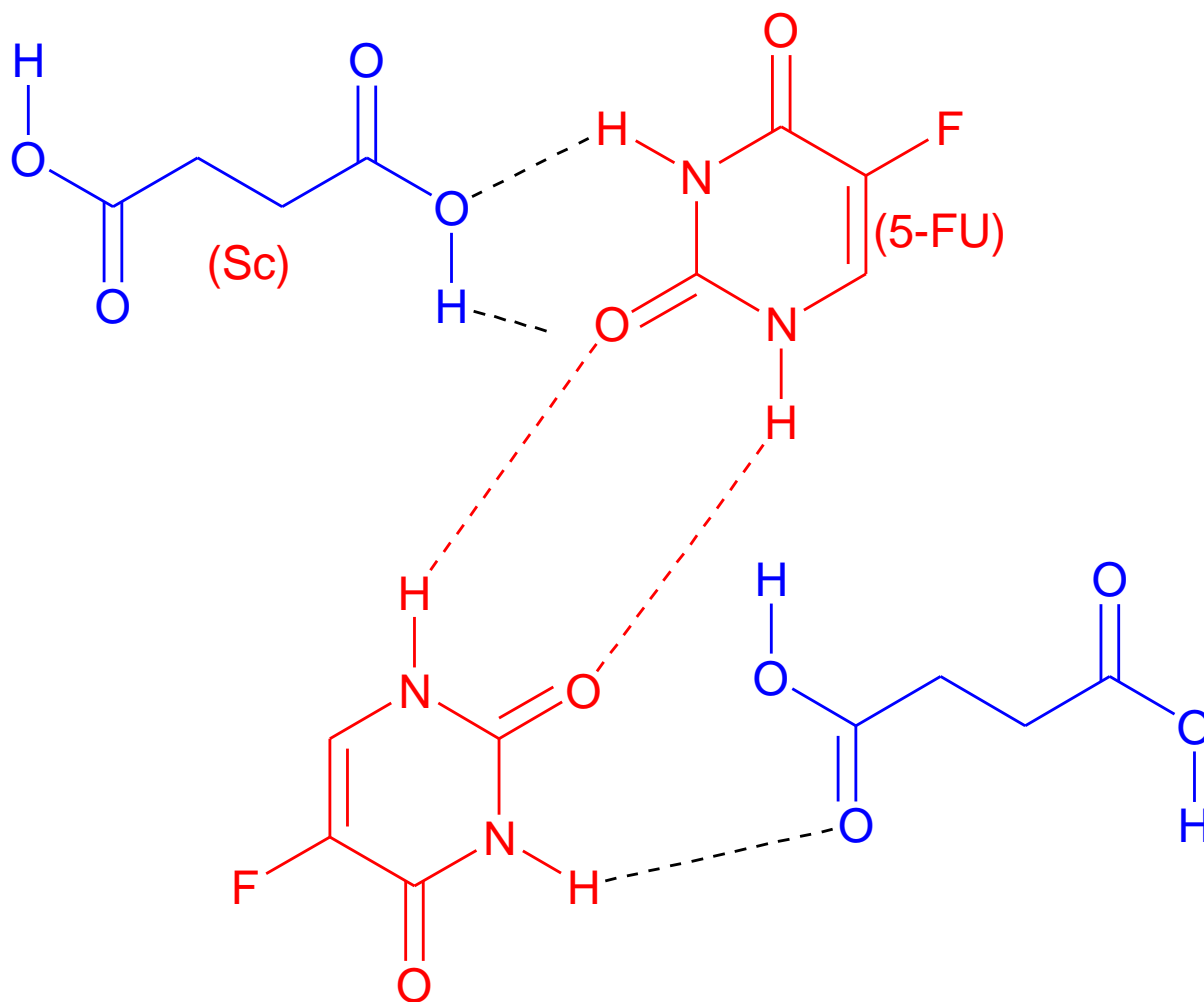
501
502
503
504



505
506
507

Figure 3. IR spectra of 5-FU, Sc (Succinic acid) co-former and 5-FU-Sc co-crystals.

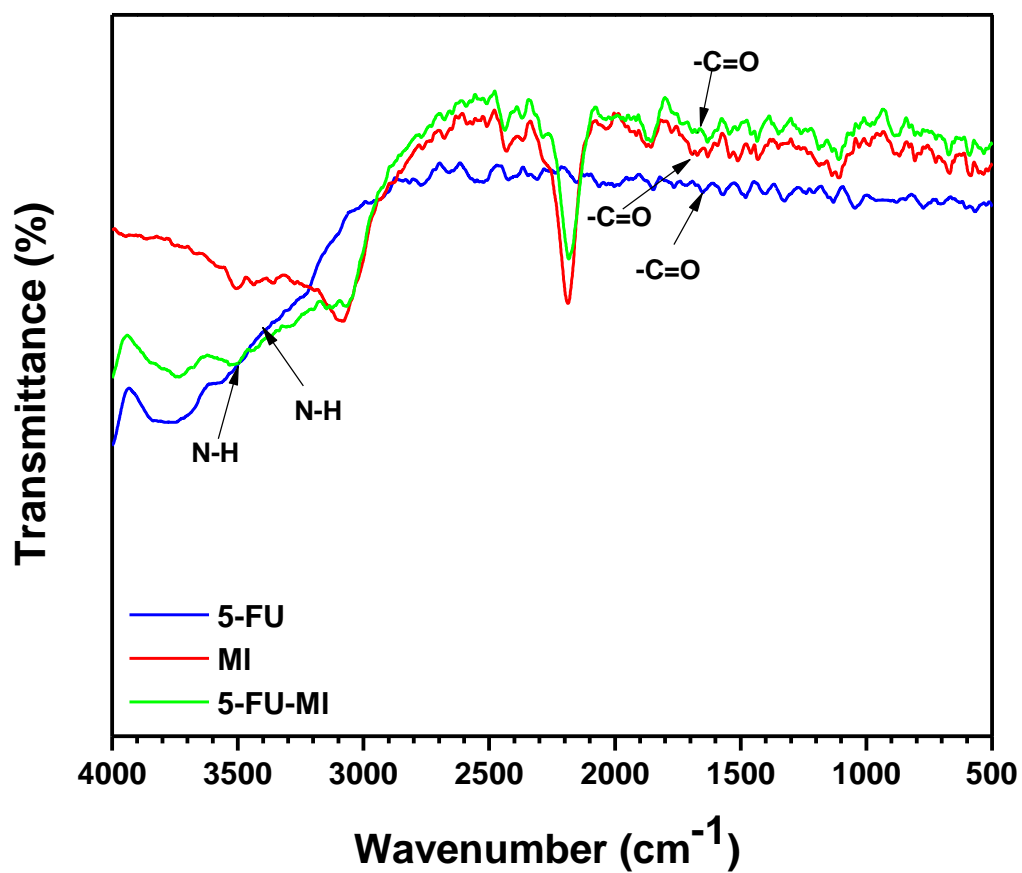
508
509
510
511
512



513
514
515

Figure 4. Proposed supramolecular interactions in 5-FU-Sc co-crystals.

516
517
518
519
520



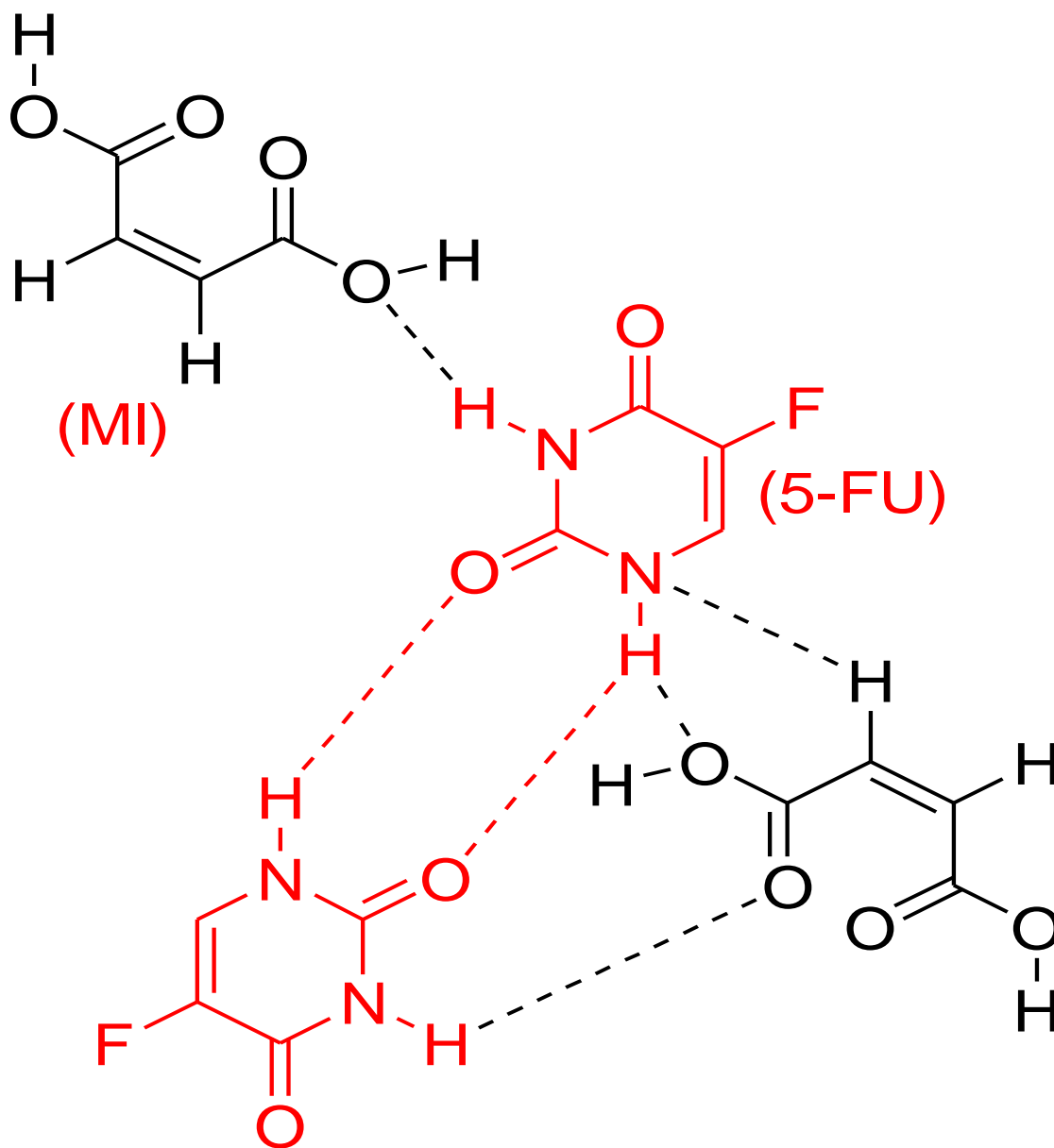
521
522
523

Figure 5. IR spectra of 5-FU, MI (Malic acid) co-former and 5-FU-MI co-crystals.

524

525

526



527

528

529

530

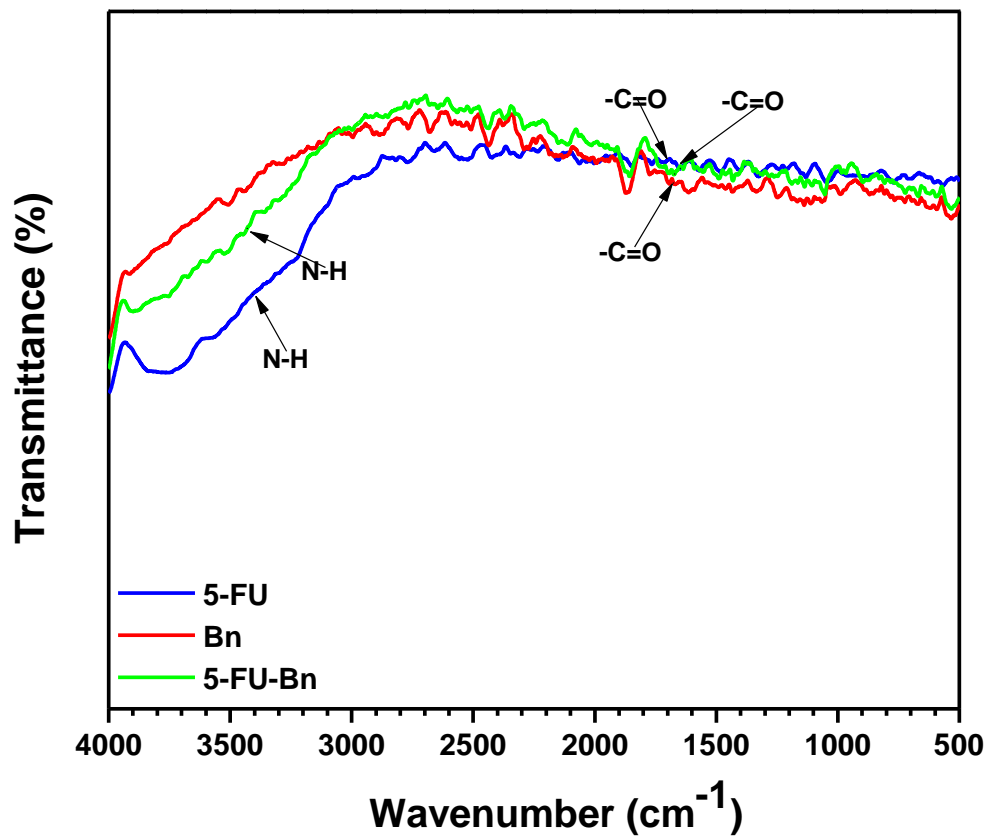
Figure 6. Proposed supramolecular interactions in 5-FU-MI co-crystals.

531

532

533

534



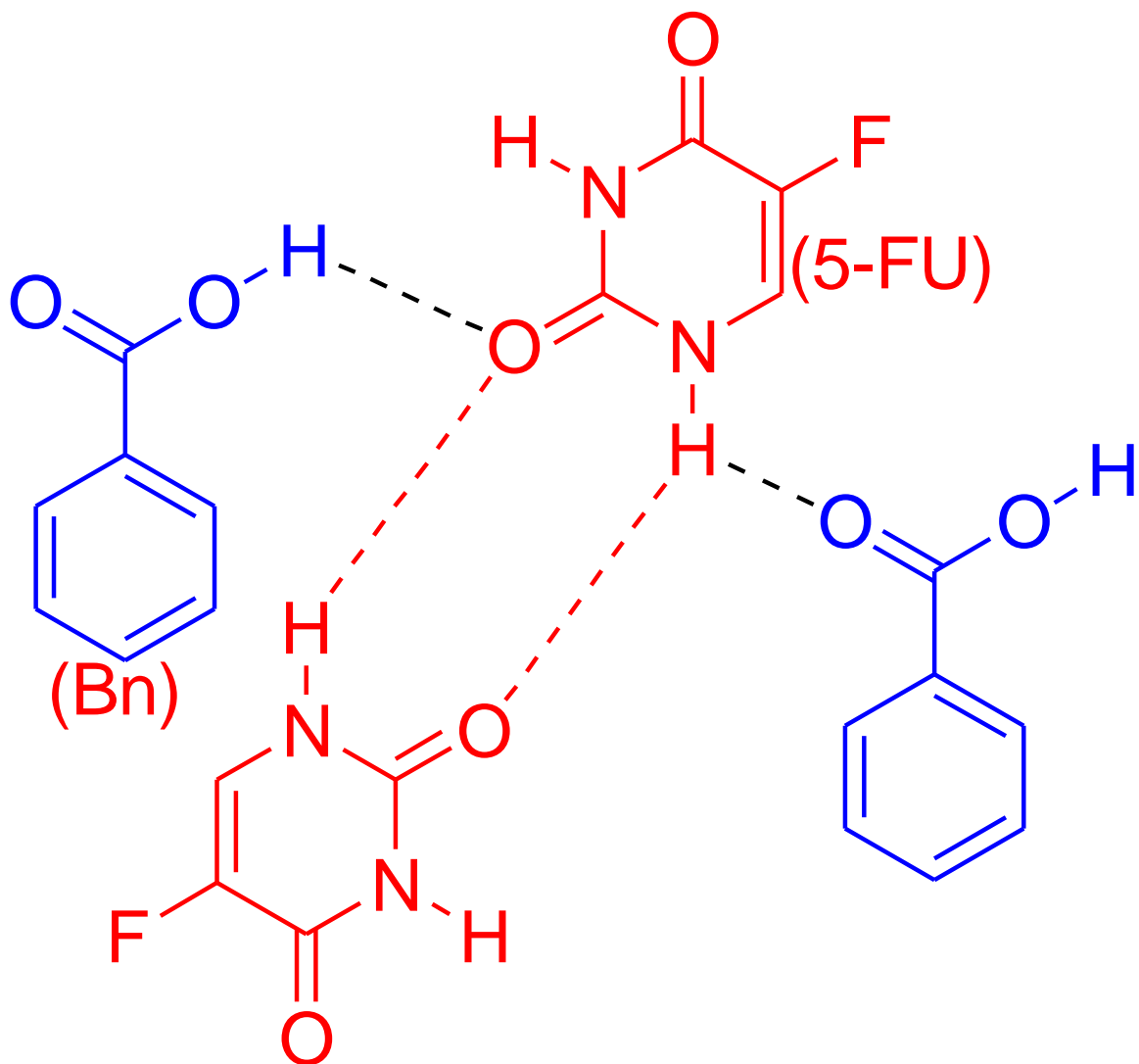
535

536 **Figure 7.** IR spectra of 5-FU, Bn (Benzoic acid) co-former and 5-FU-Bn co-crystals.

537

538

539

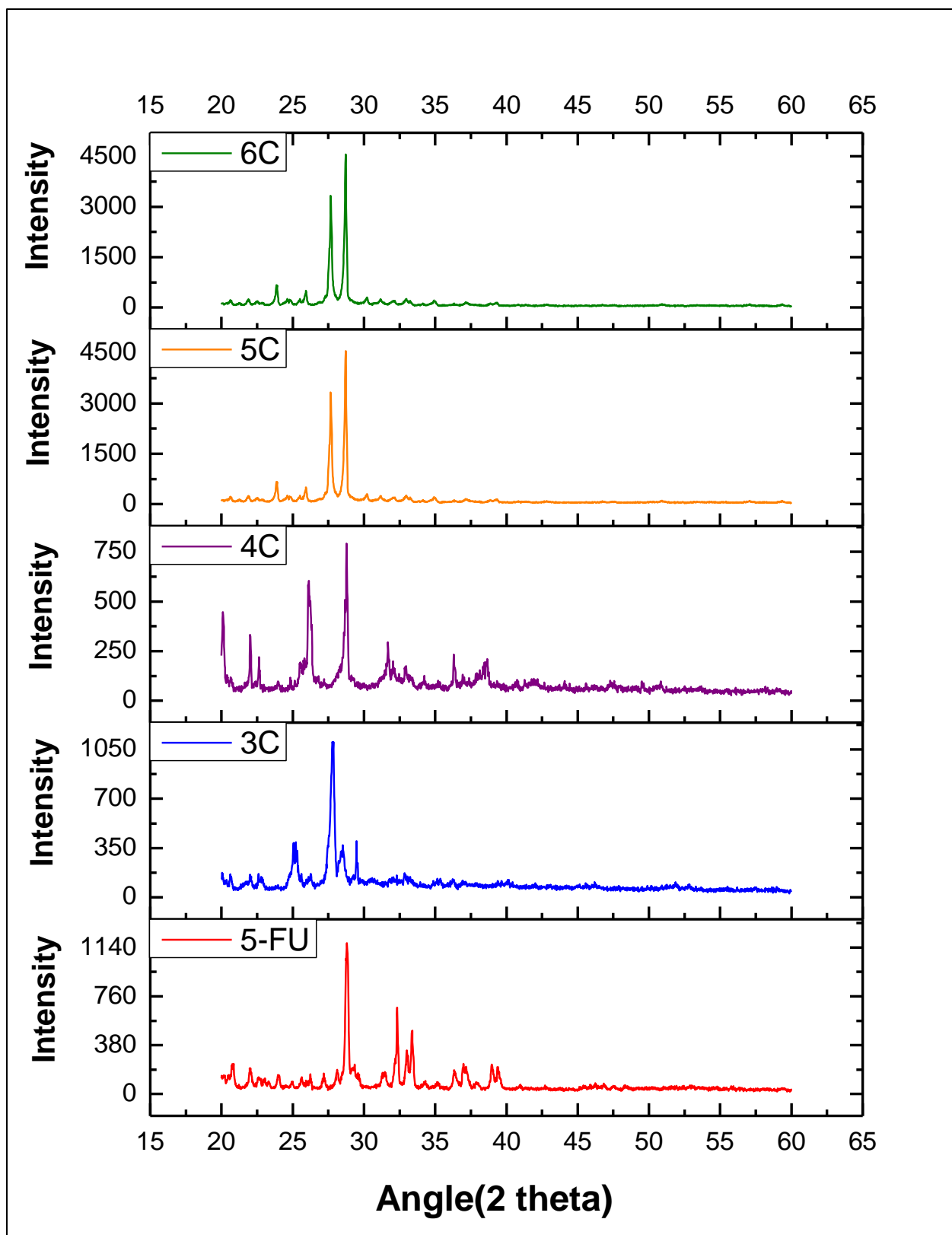


540

541

542

Figure 8. Proposed supramolecular interactions in 5-FU-Bn co-crystals.

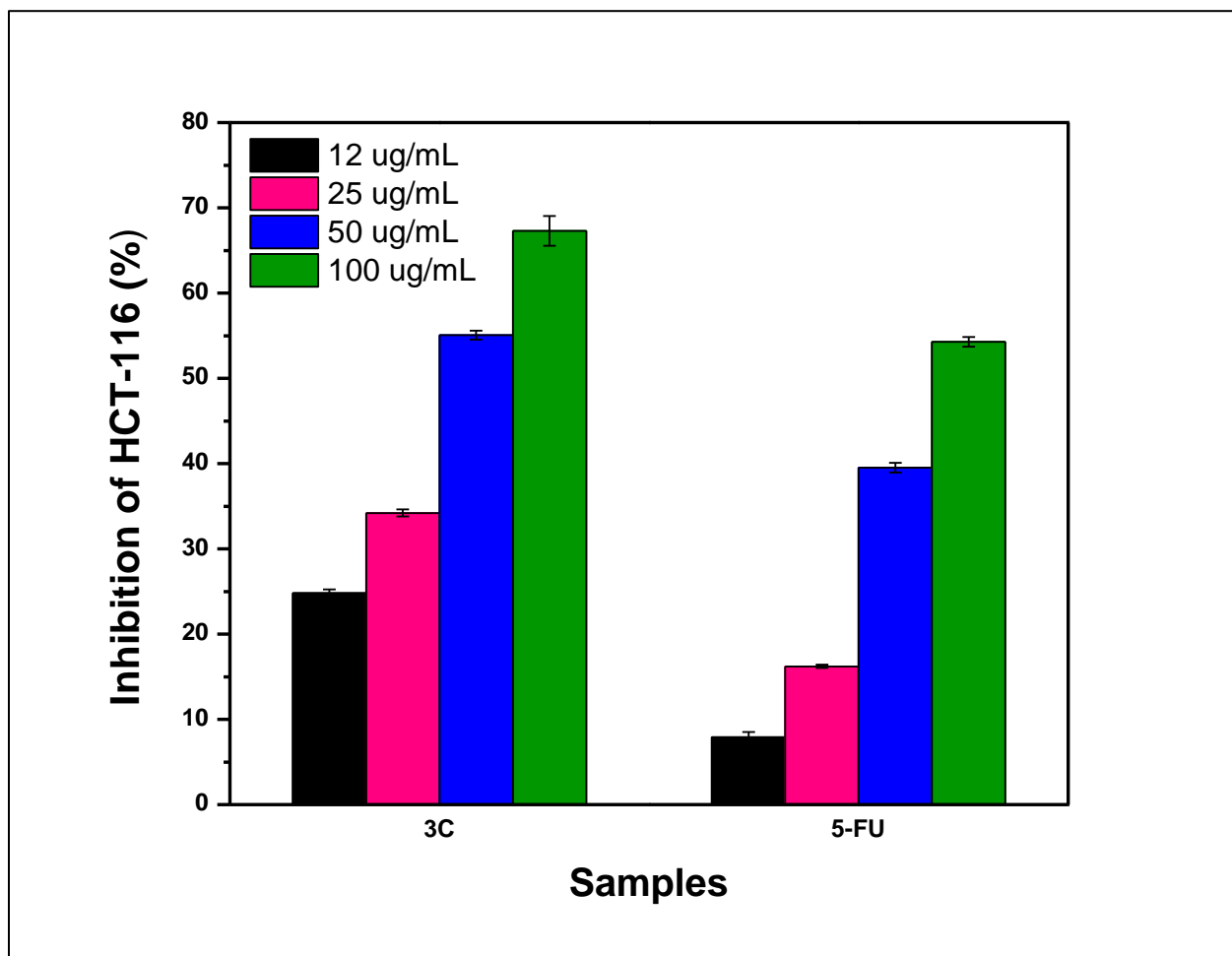


543

544

Figure 9. PXRD spectra of API and co-formers.

545
546
547
548
549



550
551
552
553

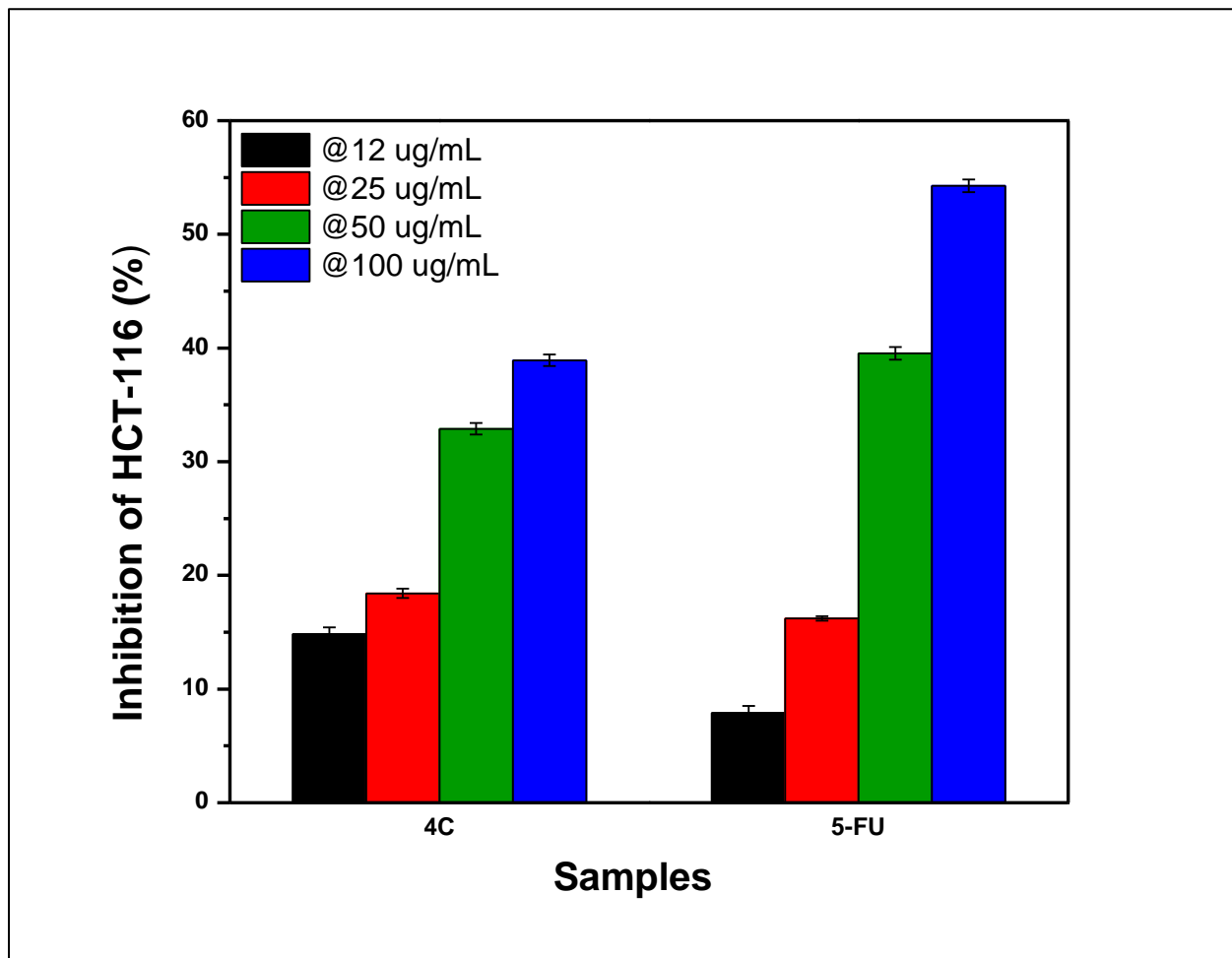
Figure 10. Comparison of percentage growth inhibition of 5-FU-Cn co-crystals with 5-FU alone at varying concentrations of API and synthesized co-crystals against HCT-116 colorectal cell lines.

554

555

556

557



558

559 **Figure 11.** Comparison of percentage growth inhibition of 5-FU-Sc co-crystals with 5-FU alone
560 at varying concentrations of API and synthesized co-crystals against HCT-116 colorectal cell lines.

561

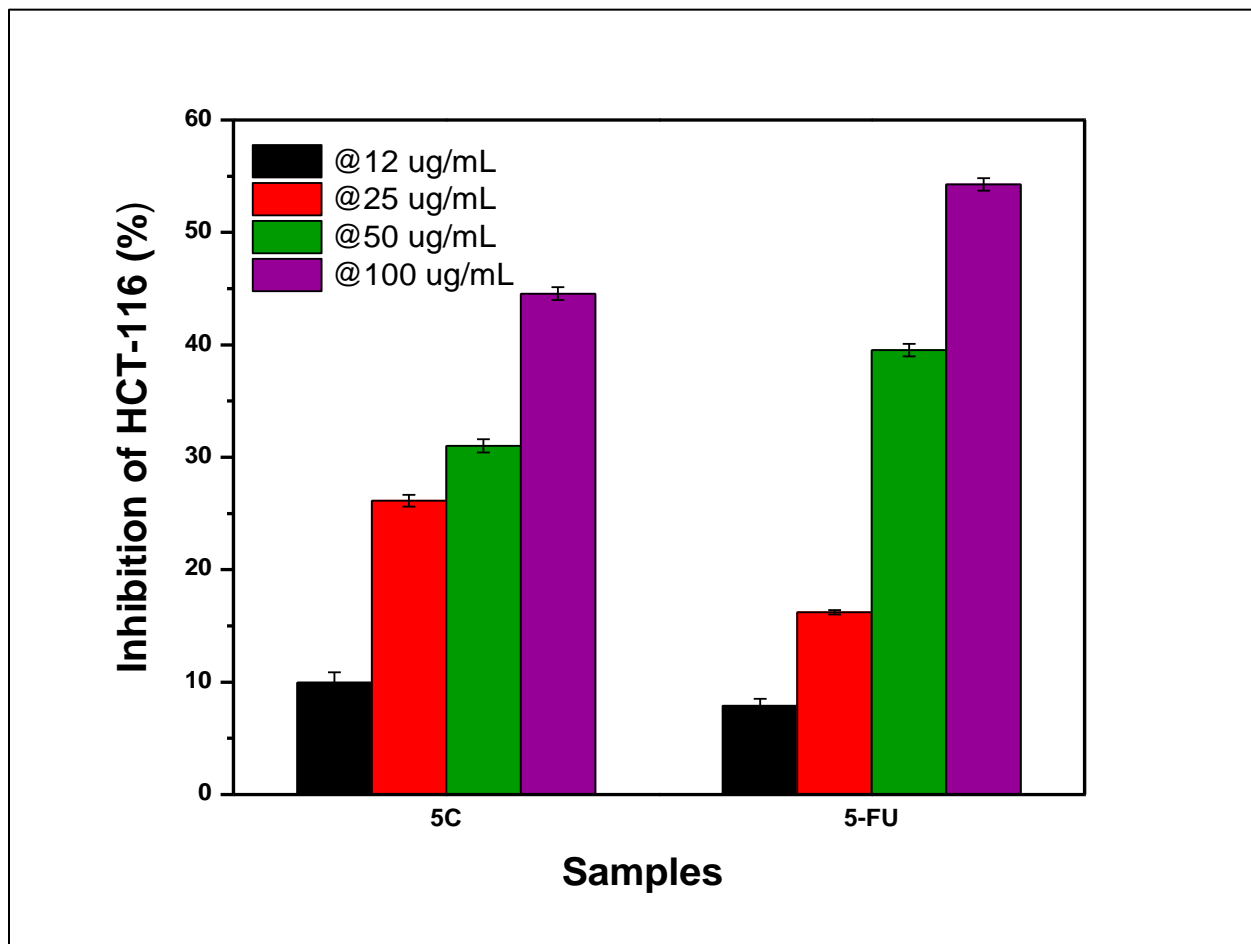
562

563

564

565

566



567

568 **Figure 12.** Comparison of percentage growth inhibition of 5-FU-MI co-crystals with 5-FU alone
569 at varying concentrations of API and synthesized co-crystals against HCT-116 colorectal cell lines.

570

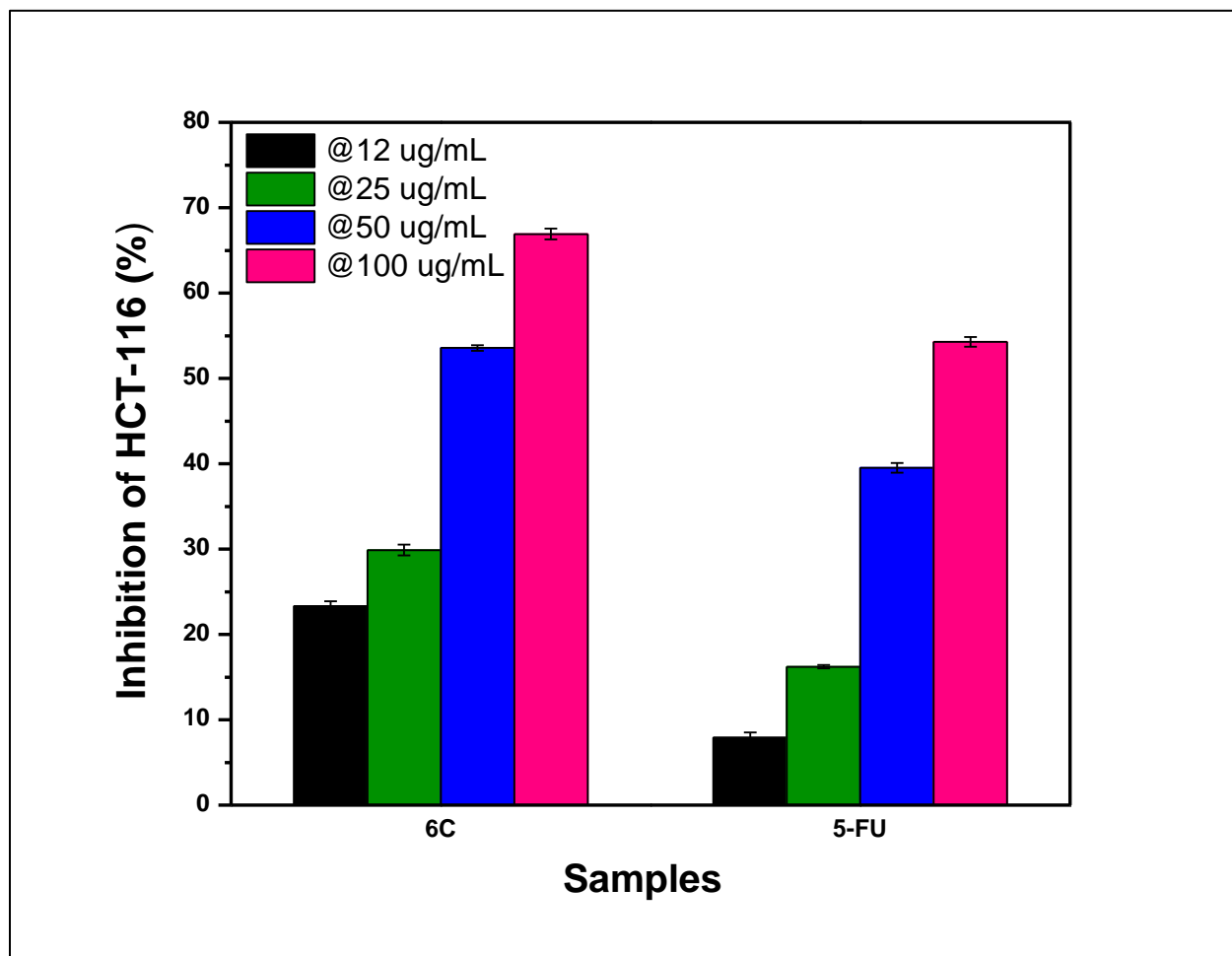
571

572

573

574

575



576

577 **Figure 13.** Comparison of percentage growth inhibition of 5-FU-Bn co-crystals with 5-FU alone
578 at varying concentrations of API and synthesized co-crystals against HCT-116 colorectal cell lines.

579

580

Table of Contents

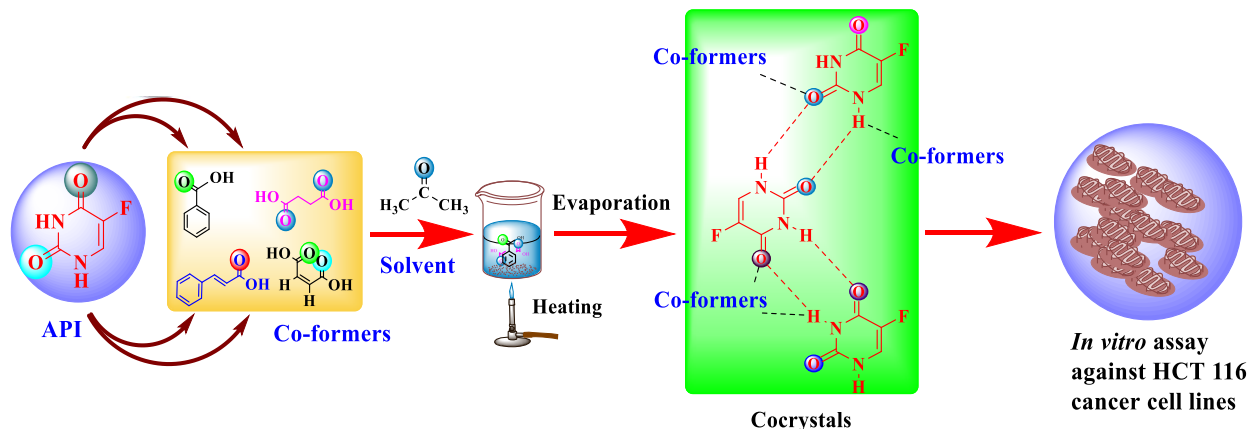
581 **Synthesis of 5-fluorouracil co-crystals with novel organic acid as co-formers** 582 **and its anticancer evaluation against HCT-116 colorectal cell lines**

583
584 Farhat Jubeen, Aisha Liaqat, Fiza Amjad, Misbah Sultan, Sania Zafar Iqbal, Imran Sajid,
585 Muhammad Bilal Khan Niazi, Farooq Sher

586

587

588



589

590

591 Co-crystallization technique to develop prodrugs of 5-Flourouracil with four organic acids:
592 Succinic acid, cinnamic acid, malic acid and benzoic acid was adopted. Characterization and
593 anticancer potential of the synthesized crystalline prodrugs were accomplished through FTIR,
594 PXRD and MTT assay against HCT-116 colorectal cell lines. All interactions in synthesized
595 prodrugs developed following vander walls interactions and exhibited greater cytotoxicity than 5-
596 Flourouracil.

597

598